PHYSICAL REVIEW B **80**, 161401(R) (2009)

Charge transfer and screening effects in polyynes encapsulated inside single-wall carbon nanotubes

L. G. Moura,[1] L. M. Malard,[1] M. A. Carneiro,[2] P. Venezuela,[2] Rodrigo B. Capaz,[3] D. Nishide,[4] Y. Achiba,[5] H. Shinohara,[4] and M. A. Pimenta[1]

[1]*Departamento de Física, Universidade Federal de Minas Gerais, 30123-970 Belo Horizonte, MG, Brazil*

[2]*Instituto de Física, Universidade Federal Fluminense, 24210-346 Niterói, RJ, Brazil*

[3]*Instituto de Física, Universidade Federal do Rio de Janeiro, Caixa Postal 68528, 21941-972 Rio de Janeiro, RJ, Brazil*

[4]*Department of Chemistry, Nagoya University, Nagoya 464-8602, Japan*

[5]*Department of Chemistry, Tokyo Metropolitan University, Hachioji 192-0397, Japan*

(Received 21 August 2009; published 2 October 2009)

A resonance Raman study of $C_{10}H_2$ and $C_{12}H_2$ polyynes encapsulated in single-wall carbon nanotubes of different diameters is presented. We show that the energy of the optical transitions associated with excited dark states of the polyyne depends on the diameter of the nanotube, as a consequence of different dielectric screenings. Strong changes in the shape of the *G* band of the metallic nanotubes are observed when they are encapsulating the carbon linear chains, reflecting charge transfers between these two systems. From *ab initio* calculations, we find that such electronic transfers are most likely occurring from the nanotubes to the polyyne molecules.

DOI: 10.1103/PhysRevB.80.161401 PACS number(s): 73.22.−f, 36.20.Ng, 78.30.Na, 78.67.Ch

Polyynes are linear carbon chains terminated by other kinds of atoms or chemical groups, such as the hydrogen terminated polyyne chain $C_{2n}H_2$ $(n \geq 2)$.[1–3] They are ideal systems to understand sp-hydrized carbon structures and to study electronic correlation effects in one-dimensional systems with potential applications in nanoelectronics. Polyynes are very unstable and the high reactivity between unsaturated sp chains tends to cause an evolution from sp to sp^2 carbon structures.[3] Interestingly, they become stable even at high temperatures when encapsulated inside single-wall carbon nanotubes (SWNTs), allowing thus easier experimental works.[1,4] However, the electronic structures of both polyynes and carbon nanotubes are extremely susceptible to environmental interactions. We will show in this work that nanotubes with different diameters provide different dielectric screening for the polyynes. Moreover, electron transfer from the nanotubes to the polyynes is evidenced by the renormalization of the nanotube phonon energies due to changes in the Fermi level.

In a previous work, Malard *et al.*[5] performed a resonance Raman study of two kinds of polyynes ($C_{10}H_2$ and $C_{12}H_2$) trapped inside SWNTs using many different laser energies in the visible range, and observed that the intensity of the Raman band associated with the stretching modes of the polyynes inside SWNTs is strongly enhanced for laser energies around 2.10 eV. The energy of this resonance is much lower than the energy of the absorption peaks of $C_{10}H_2$ and $C_{12}H_2$ polyynes in organic solvents (4.9 and 4.5 eV, respectively) or in gas phase (5.4 and 5.0 eV, respectively). This observed resonance was assigned to dipole-forbidden ("dark") transitions becoming allowed due to symmetry breaking, when the polyynes are displaced from the axis of the tube.[5] DFT calculations estimated that the energy of these "dark" states are between 2 and 3 eV, in agreement with the Raman measurements.

In this Rapid Communication, we present a resonance Raman study of $C_{10}H_2$ and $C_{12}H_2$ polyynes trapped inside single-wall carbon nanotubes of different diameters, using many different laser energies in the visible range. We show that the polyyne resonance energies decrease with increasing diameter of the nanotubes, as a consequence of changes in the screening from the tubes of different diameters. We also observe a redshift and strong changes in the shape of the *G* band of the metallic nanotubes when they encapsulate polyynes, reflecting charge transfers between these two systems. These charge transfers are interpreted using *ab initio* calculations.

The preparation of the polyynes inside nanotube samples is described in Refs. 1, 6, and 7. Before the encapsulation treatment, SWNTs were purified by the H_2O_2/HCl treatment and thermal oxidation, and the SWNTs/polyyne/hexane solution was degassed by freeze-thaw process. Therefore, no chemical functionalization is expected to occur during the purification processes. The Raman measurements were performed in aggregates of nanotube bundles. The diameters of the nanotubes were estimated from the radial breathing modes (RBMs) Raman spectra[8] using the relation $d = A/(\omega_{RBM} - B)$, where ω_{RBM} is the RBM frequency, and $A = 219$ cm^{-1} nm and $B = 15$ cm^{-1}.[8] The samples with average large, medium, and small diameters were labeled as L($d = 1.45 \pm 0.15$ nm), M($d = 1.35 \pm 0.15$ nm), and S($d = 1.2 \pm 0.1$ nm), respectively.

Raman-scattering experiments were performed at room temperature using a triple monochromator micro-Raman spectrometer Dilor XY. An Ar-Kr and a dye laser were used and experiments were performed using many lasers lines in the visible range from 1.92 to 2.71 eV (647 to 457.9 nm). The laser power used was around 1 mW with a spot diameter of 1 μm using a 80× objective.

Ab initio calculations based on density-functional theory[9,10] (DFT) were used to obtain the structural and electronic properties of pristine and polyyne-encapsulated SWNTs. The calculations were performed by the SIESTA code,[11] which performs self-consistent calculations solving

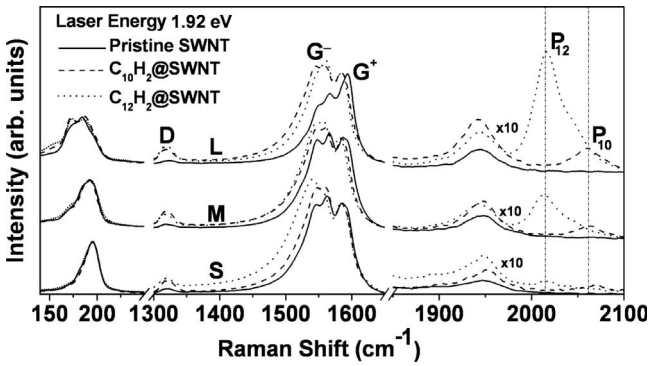

FIG. 1. Raman spectra using the 1.92 eV excitation energy for pristine SWNTs (solid curves), $C_{10}H_2$@SWNT (dashed curves), and $C_{12}H_2$@SWNT (dotted curves) showing the RBM modes, the *G* band between 1500 and 1600 cm^{-1} and the polyynes bands indexed by P_{12} and P_{10} between 2000 and 2100 cm^{-1}. The labels L, M, and S denote SWNTs with large, medium, and small diameters, respectively.

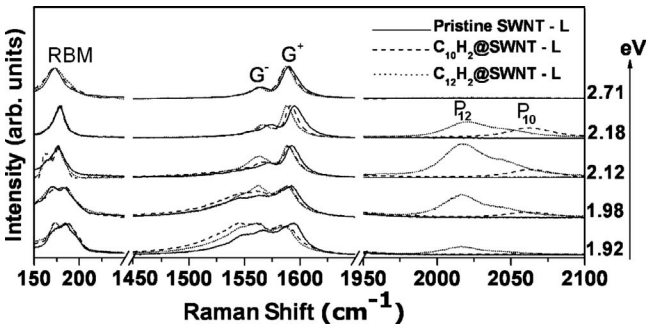

FIG. 2. Raman spectra of the pristine SWNT and the $C_{10}H_2$@SWNT and $C_{12}H_2$SWNT samples with larger nanotube diameter, recorded using different laser energies (1.92, 1.98, 2.12, 2.18, and 2.71 eV), showing the RBM and *G* bands of the SWNTs and the *P* band of the polyynes.

the Kohn-Sham equations by means of numerical atomic-orbital basis sets. We used double-zeta basis sets plus polarization functions, the local-density approximation (LDA) (Ref. 12) for the exchange-correlation potential, and norm conserving Troullier-Martins pseudopotentials.[13] Periodic boundary conditions were used so that the lateral separation between tube centers are 4 nm and the total length of the tubes are 2.224 nm. This choice prevents spurious interactions between polyyne molecules along the axial direction. Brillouin-zone sampling has been made with four Monkhorst-Pack points in the longitudinal direction of the nanotube.[14] A cutoff of 150 Ryd for the grid integration is utilized to represent the charge density. All systems studied here are structurally relaxed until the residual forces were smaller than 0.05 eV/Å. Calculations were performed for different polyyne molecules encapsulated in the (5,5) SWNT. Test calculations with the generalized gradient approximation,[15] double-zeta basis sets and a larger diameter nanotube, namely the (8,8) SWNT, have been made in order to assure that our main results do not depend on the functional type, basis sets, and diameter of the tube.

Figure 1 shows the Raman spectra for the nine samples investigated in this work, using the 1.92 eV laser energy. The solid, dashed, and dotted line spectra correspond to pristine SWNT, $C_{10}H_2$@SWNT, and $C_{12}H_2$@SWNT samples, respectively; and the indexes L, M, and S refer to large, medium, and small nanotube diameters, respectively. The intensity of the G^+ peak was used for normalizing all spectra. Figure 1 shows three important features of the Raman spectra of carbon nanotubes, the RBMs between 150 and 220 cm^{-1}, the *D* band associated with disorder or defects, around 1300 cm^{-1}, and the *G* band around 1590 cm^{-1} that corresponds to the tangential vibrational modes. The *G* band of carbon nanotubes splits into two prominent peaks, assigned as G^- and G^+,[16] associated with the TO (transverse-optical) and LO (longitudinal-optical) phonon modes of the semiconducting nanotubes, respectively. In the case of metallic nanotubes, due to the presence of Kohn anomaly, the LO and TO modes are assigned to the G^- and G^+ peaks, respectively.[17,18] Notice that both the position and the shape of the *G* band change when the nanotubes are encapsulating the polyynes.

In Fig. 1, we can also observe a band around 1950 cm^{-1}, which is due to a double-resonance second-order Raman feature characteristic of all graphitic systems.[19] The bands between 2000 and 2100 cm^{-1} indexed by *P* are associated with the stretching modes of the polyynes.[4,20,21] The peaks around 2018 and 2064 cm^{-1} assigned as P_{12} and P_{10}, are associated with the stretching vibrational modes of the $C_{12}H_2$ and $C_{10}H_2$ molecules, respectively. Notice in Fig. 1 that the polyynes bands are more intense for nanotubes with larger diameters. This result is consistent with the explanation that the resonant behavior of this peak is associated with dark exited states of the polyynes, activated by symmetry breaking when the chains are displaced from the central axis of the nanotubes.[5] Symmetry breaking is expected to be stronger for larger diameter nanotubes.

Figure 2 shows the Raman spectra of the pristine SWNT-L, $C_{10}H_2$@SWNT-L, and $C_{12}H_2$@SWNT-L samples recorded with different laser energies. We can observe that the P_{10} and P_{12} peaks intensity are strongly enhanced for laser energies between 2.1 and 2.2 eV. A similar behavior is observed for all other polyyne samples investigated in this work. Figure 3 shows the integrated intensity of the *P* band as a function of the laser excitation energy, fitted by Gaussian functions, for $C_{10}H_2$ and $C_{12}H_2$ trapped inside SWNTs of different diameters. This resonance behavior is due to the optical transitions of the polyynes, associated with the "dark" states of the isolated molecules.[5] Notice that transition energies depend on the nanotube diameter for both $C_{10}H_2$@SWNT and $C_{12}H_2$@SWNT, increasing with decreasing nanotube diameter. This dependence reflects an "environment" effect on the transition energies of the molecules. It is a well-reported effect that optical transitions of molecules are usually redshifted when they are placed in a dielectric medium, known as positive (or normal) solvatochromism.[22] Larger nanotubes provide a strongest dielectric screening of the Coulomb interactions, therefore increasing the redshift. This effect occurs for both semiconducting and metallic nanotubes because, in either case, tubes with larger diameters have a larger number of virtual sub-

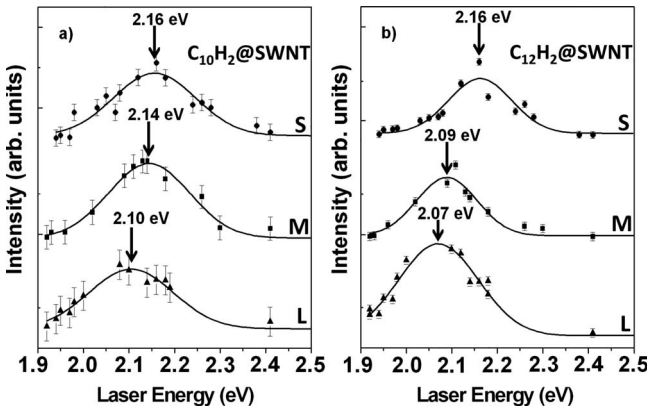

FIG. 3. Raman intensity of the P bands for $C_{10}H_2$ and $C_{12}H_2$ as a function of the laser excitation energy, for single-wall carbon nanotubes of different diameters.

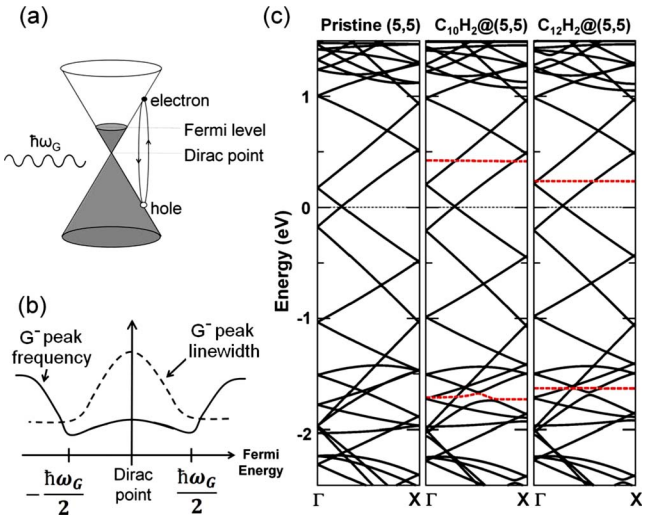

FIG. 4. (Color online) (a) Phonon assisted creation and annihilation of an electron-hole pair. (b) Frequency (full line) and the linewidth (dashed line) of the G^- peak of metallic nanotubes as a function of the Fermi-level position (Refs. 28 and 30). (c) Electronic band structure for the pristine (5,5) SWNT (left), $C_{10}H_2$@(5,5) (middle), and $C_{12}H_2$(5,5) (right). The highest-unoccupied-molecular-orbital (HOMO) and lowest-unoccupied-molecular-orbital (LUMO) bands of the polyyne molecules are shown in dashed red lines. The dotted line is the Fermi level for undoped samples.

band transitions to contribute to screening. We can also observe in Fig. 3 that the resonance energy is generally lower for $C_{12}H_2$ than $C_{10}H_2$. This result is in agreement with DFT calculations that estimate a lower resonance energy for $C_{12}H_2$ than $C_{10}H_2$.[5] Moreover a similar behavior can be observed in the absorption spectra.[2,21]

The effect of polyynes on the G band of the nanotubes can be also observed in Fig. 2, which shows the G band for the large diameter sample, measured with different laser energies. A similar behavior is observed for the nanotube samples with medium and small diameters. The solid, dashed and dotted curves correspond to pristine SWNTs, $C_{10}H_2$@SWNT, and $C_{12}H_2$@SWNT, respectively. In the two upper spectra in Fig. 2 (2.18 and 2.71 eV), the shape of G band does not change when the nanotubes are encapsulating the polyynes; we can only observe a downshift of the whole band. However, important changes in the shape of the G band are observed in the three lower spectra in Fig. 2 (2.12, 1.98, and 1.92 eV), where a significant broadening and decrease of the G^- component for the encapsulated samples is observed.

In order to explain the changes in the G band measured with different laser energies shown in Fig. 2, we need to consider the diameter dependence of the optical transitions of the nanotubes. Considering the range of nanotube diameters (1.1–1.5 nm) and the range of laser energies (1.92–2.71 eV) used in this work, we can conclude from the Kataura plot[23] that the spectra in Fig. 2 obtained using lower laser energies (1.92 and 1.98 eV) show predominantly the metallic nanotubes, since these energies are in resonance with the E_{11}^M transitions of the metallic nanotubes present in the samples.[24] The spectra recorded with higher laser energies (2.18 and 2.71 eV) show the contribution of the semiconducting nanotubes, in resonance with the E_{33}^S transitions. The spectrum at 2.12 eV shows the contribution of both the metallic and semiconducting nanotubes. Thus, it can be concluded that the drastic changes in the shape of the G band in Fig. 2 occur for metallic nanotubes encapsulating polyyne molecules.

The G band of metallic nanotubes exhibits a broad and asymmetric shape and it is very sensitive to environment and to charge transfers.[24,25] Some authors attributed this shape to coupled excitations involving plasmon and phonons, that should occur in the case of nanotubes in bundles or in contact with a substrate.[26,27] Recently, it has been proposed that the broad G band is due to electron-phonon coupling in metallic nanotubes (Kohn anomaly) of small chiral angle[18,28–30] and occur even in the case of isolated nanotubes.[29]

In this work, the strong effect of the polyynes on the shape of G^- peak of the metallic nanotubes is interpreted in terms of the changes in the Fermi level and its effect on the electron-phonon coupling. It was recently shown by different authors[18,28–30] that the position and linewidth of the G^- peak of the metallic nanotubes is strongly dependent on the Fermi-level position due to the phonon-assisted electron-hole pair-creation process schematically shown in Fig. 4(a), which gives rise to the Kohn anomaly. The renormalization of the G phonon energy due to this process can be obtained from a time-dependent perturbation theory,[18,28,30] and the dependence of the frequency (full line) and linewidth (dashed line) of the G^- peak as a function of Fermi level is shown in Fig. 4(b).[28–30] When the changes in the Fermi level are higher than half of the phonon energy, the electron-hole pair-creation process is blocked due to the Fermi exclusion principle, thus hardening the phonon frequency. Moreover, the electron-phonon coupling decreases the lifetime of the phonon, resulting in a broadening of the G peak when the Fermi level approaches the neutrality point, as shown in Fig. 4(b).

Figure 2 shows that the G^- peak of the metallic nanotubes downshifts and broadens when they are encapsulating the polyynes. Considering the electron-phonon process discussed above, we conclude that the Fermi level of the metallic pristine nanotubes samples is not at the Dirac point, since the neutrality point would correspond to the maximum

G-band broadening. This result suggests an intrinsic doping of the pristine sample. When the polyynes are encapsulated inside nanotubes, charge transfers occur between the two system, changing the Fermi level of the metallic nanotubes toward the Dirac point, softening and broadening the *G* band.

In order to understand in more detail the charge-transfer process between polyyne molecules and metallic nanotubes, we performed *ab initio* calculations of a pristine (5,5) and encapsulated $C_{10}H_2$@(5,5) and $C_{12}H_2$@(5,5) systems. The Kohn-Sham electronic band structures for the three cases are shown in Fig. 4(c). One clearly sees that the electronic HOMO and LUMO states of both $C_{10}H_2$ and $C_{12}H_2$ have very little hybridization with the electronic states of the nanotube, indicating that the composite system is very weakly interacting from a chemical point of view. Charge transfer between the molecule and the tube can occur only if the Fermi level of the pristine (5,5) tube is either *above* the LUMO or *below* the HOMO of the molecules. This is not the case for undoped systems, as one can see. However, residual doping could lead, in principle, to either one of these two cases. However, one sees that the LUMO states are much closer to the nondoped Fermi energy than HOMO states. For instance, for the $C_{12}H_2$@(5,5) system, the LUMO is only 0.2 eV above the undoped Fermi level, whereas the HOMO is 1.6 eV below it. Therefore, since we do not expect a large residual doping in our samples, the first situation, corresponding to a small *n*-type doping of the pristine samples, is more plausible to occur. For this reason, we propose that electrons are transferred from the nanotubes to the molecules upon encapsulation. This result is in agreement with the recent DFT calculations performed by Kertesz and Yang.[31]

In summary, this work presents a resonance Raman study of $C_{10}H_2$ and $C_{12}H_2$ polyynes inside single-wall carbon nanotubes of different diameters, using many different laser energies in the visible range. We show that there is a dependence of the optical transition energies of the polyyne molecules with respect to the diameter of nanotubes, the energy decreasing with increasing diameter of the nanotubes. This environment effect is understood as a normal solvatochromic shift due to variations in the dielectric screening of the tubes. We have also observed a redshift and strong changes in the shape of the *G* band of the metallic nanotubes when they encapsulate the polyynes and, this result was interpreted in terms of changes in the electron-phonon coupling due to charge transfer between the polyynes and the tubes. From *ab initio* calculations, we conclude that this electronic transfer is most likely occurring from the tubes to the molecules.

This work was supported by Rede Nacional de Pesquisa em Nanotubos de Carbono-MCT, and Brazilian agencies FAPEMIG, FAPERJ and CNPq.

[1] D. Nishide *et al.*, Chem. Phys. Lett. **428**, 356 (2006).
[2] H. Tabata *et al.*, Carbon **44**, 3168 (2006).
[3] F. Cataldo, *Polyynes: Synthesis, Properties, and Applications* (Taylor & Francis Group, LLC, Boca Raton, London, New York, 2006) pp. 16, 128, 156, and 157.
[4] D. Nishide *et al.*, J. Phys. Chem. C **111**, 5178 (2007).
[5] L. M. Malard *et al.*, Phys. Rev. B **76**, 233412 (2007).
[6] M. Tsuji *et al.*, Chem. Phys. Lett. **355**, 101 (2002).
[7] D. Nishide *et al.*, Chem. Phys. Lett. **372**, 45 (2003).
[8] C. Fantini, A. Jorio, M. Souza, M. S. Strano, M. S. Dresselhaus, and M. A. Pimenta, Phys. Rev. Lett. **93**, 147406 (2004).
[9] P. Hohenberg and W. Kohn, Phys. Rev. **136**, B864 (1964).
[10] W. Kohn and L. J. Sham, Phys. Rev. **140**, A1133 (1965).
[11] J. M. Soler *et al.*, J. Phys.: Condens. Matter **14**, 2745 (2002).
[12] J. P. Perdew and A. Zunger, Phys. Rev. B **23**, 5048 (1981).
[13] N. Troullier and J. L. Martins, Phys. Rev. B **43**, 1993 (1991).
[14] H. J. Monkhorst and J. D. Pack, Phys. Rev. B **13**, 5188 (1976).
[15] J. P. Perdew, K. Burke, and M. Ernzerhof, Phys. Rev. Lett. **77**, 3865 (1996).
[16] A. Jorio *et al.*, Phys. Rev. B **65**, 155412 (2002).
[17] S. Piscanec, M. Lazzeri, J. Robertson, A. C. Ferrari, and F. Mauri, Phys. Rev. B **75**, 035427 (2007).
[18] M. Lazzeri, S. Piscanec, F. Mauri, A. C. Ferrari, and J. Robertson, Phys. Rev. B **73**, 155426 (2006).
[19] V. W. Brar, G. G. Samsonidze, M. S. Dresselhaus, G. Dresselhaus, R. Saito, A. K. Swan, M. S. Unlu, B. B. Goldberg, A. G. Souza Filho, and A. Jorio, Phys. Rev. B **66**, 155418 (2002).
[20] T. Wakabayashi *et al.*, Chem. Phys. Lett. **433**, 296 (2007).
[21] T. Wakabayashi *et al.*, Chem. Phys. Lett. **446**, 65 (2007).
[22] C. Reichardt, Chem. Rev. (Washington, D.C.) **94**, 2319 (1994).
[23] A. Jorio *et al.*, Phys. Rev. B **71**, 075401 (2005).
[24] M. A. Pimenta, A. Marucci, S. A. Empedocles, M. G. Bawendi, E. B. Hanlon, A. M. Rao, P. C. Eklund, R. E. Smalley, G. Dresselhaus, and M. S. Dresselhaus, Phys. Rev. B **58**, R16016 (1998).
[25] J. Cardenas, Carbon **46**, 1327 (2008).
[26] C. Jiang, K. Kempa, J. Zhao, U. Schlecht, U. Kolb, T. Basche, M. Burghard, and A. Mews, Phys. Rev. B **66**, 161404(R) (2002).
[27] S. D. M. Brown, A. Jorio, P. Corio, M. S. Dresselhaus, G. Dresselhaus, R. Saito, and K. Kneipp, Phys. Rev. B **63**, 155414 (2001).
[28] K. I. Sasaki, R. Saito, G. Dresselhaus, M. S. Dresselhaus, H. Farhat, and J. Kong, Phys. Rev. B **77**, 245441 (2008).
[29] Y. Wu, J. Maultzsch, E. Knoesel, B. Chandra, M. Huang, M. Y. Sfeir, L. E. Brus, J. Hone, and T. F. Heinz, Phys. Rev. Lett. **99**, 027402 (2007).
[30] J. C. Tsang *et al.*, Nat. Nanotechnol. **2**, 725 (2007).
[31] M. Kertesz and S. Yangw, Phys. Chem. Chem. Phys. **11**, 425 (2009).